Hindawi
Advances in Mathematical Physics
Volume 2019, Article ID 1030318, 9 pages
https://doi.org/10.1155/2019/1030318

Research Article

Numerical Simulation of the Lorenz-Type Chaotic System Using Barycentric Lagrange Interpolation Collocation Method

Jun-Mei Li,[1] Yu-Lan Wang ,[1] and Wei Zhang [2]

[1] *Department of Mathematics, Inner Mongolia University of Technology, Hohhot 010051, China*
[2] *Institute of Economics and Management, Jining Normal University, Jining 012000, Inner Mongolia, China*

Correspondence should be addressed to Yu-Lan Wang; wylnei@163.com

Received 5 December 2018; Revised 9 February 2019; Accepted 7 March 2019; Published 1 April 2019

Academic Editor: Zengtao Chen

Although some numerical methods of the Lorenz system have been announced, simple and efficient methods have always been the direction that scholars strive to pursue. Based on this problem, this paper introduces a novel numerical method to solve the Lorenz-type chaotic system which is based on barycentric Lagrange interpolation collocation method (BLICM). The system (1) is adopted as an example to elucidate the solution process. Numerical simulations are used to verify the effectiveness of the present method.

1. Introduction

In 1963, Edward Lorenz developed a simplified mathematical model for atmospheric convection. The model is a system of three ordinary differential equations now known as the Lorenz equations (see [1–3]):

$$\begin{aligned} \frac{dx}{dt} &= a(y-x), \\ \frac{dy}{dt} &= x(c-x)-y, \\ \frac{dz}{dt} &= -bz+xy, \end{aligned} \tag{1}$$

$$t \in [0,T]$$

with the initial conditions

$$\begin{aligned} x(0) &= c_1, \\ y(0) &= c_2, \\ z(0) &= c_3, \end{aligned} \tag{2}$$

where $x(t)$ is proportional to the rate of convection, $y(t)$ to the horizontal temperature variation, and $z(t)$ to the vertical temperature variation. The constants a, c, b are system parameters proportional to the Prandtl number, Rayleigh number, and certain physical dimensions of the layer itself.

As chaos theory progresses, many new Lorenz-type systems [4–6] have been proposed, specially Lorenz hyperchaotic systems [7–10]. The Lorenz system is widely used in electric circuits, chemical reactions, and forward osmosis. Although some numerical methods of the Lorenz system have been announced, simple and efficient methods have always been the direction that scholars strive to pursue.

With the development of numerical analysis, there are some high-precision methods, such as variational iteration method [11–13], BLICM [14–22], and so on [23]. J.P. Berrut [24–26] introduced barycentric Lagrange interpolation, [27, 28] studied numerical stability of barycentric Lagrange interpolation, and [15, 16] give algorithm of BLICM. Some authors [14, 17–22] have used BLICM to solve all sorts of problems and show the BLICM is a high precision numerical method. This paper suggests the BLICM to solve the Lorenz system. The system (1) is adopted as an example to elucidate the solution process.

2. The Numerical Solution of the System (1)

First of all, we give initial function $x_0(t), y_0(t), z_0(t)$ and construct following linear iterative format of system (1)

$$\begin{aligned} &\frac{dx_n}{dt} + ax_n(t) - ay_n(t) = 0, \\ &\frac{dy_n}{dt} - cx_n(t) + y_n(t) = x_{n-1}(t)\, z_{n-1}(t), \\ &\frac{dz_n}{dt} + bz_n(t) = x_{n-1}(t)\, y_{n-1}(t). \\ &n = 1, 2, 3, \ldots, \end{aligned} \tag{3}$$

Next, we use BLICM to solve (3).

Using the barycentric Lagrange interpolation functions [14–16, 24–26], we can get following:

$$\begin{aligned} x_n(t) &= \sum_{j=1}^{M} \xi_j(t)\, x_n(t_j), \\ y_n(t) &= \sum_{j=1}^{M} \xi_j(t)\, y_n(t_j), \\ z_n(t) &= \sum_{j=1}^{M} \xi_j(t)\, z_n(t_j). \end{aligned} \tag{4}$$

$$\begin{aligned} x_n'(t) &= \sum_{j=1}^{M} \xi_j'(t)\, x_n(t_j), \\ y_n'(t) &= \sum_{j=1}^{M} \xi_j'(t)\, y_n(t_j), \\ z_n'(t) &= \sum_{j=1}^{M} \xi_j'(t)\, z_n(t_j). \end{aligned} \tag{5}$$

$$\begin{aligned} &\sum_{i=1}^{M} \xi_i(0)\, x_n(t_i) = c_1, \\ &\sum_{i=1}^{M} \xi_i(0)\, y_n(t_i) = c_2, \\ &\sum_{i=1}^{M} \xi_i(0)\, z_n(t_i) = c_3. \end{aligned} \tag{6}$$

where $\xi_j(t) = (\omega_j/(t - t_j))/\sum_{k=1}^{M}(\omega_k/(t - t_k))$ is respectively barycentric interpolation primary function, $\omega_j = 1/\prod_{i=1, j\neq k}^{M}(t_i - t_j)$ is center of gravity Lagrange interpolation weight, and $0 \le t_1 < t_2 < \cdots < t_M \le T$.

Substitute formulae (4) and (5) into iterative format (3) and let $t = t_i$, $(i = 1, 2, \cdots M)$. So, linear iterative format (3) can be written in following partitioned matrix form:

$$\begin{bmatrix} D + aI & -aI & 0 \\ -cI & D + I & 0 \\ 0 & 0 & D + bI \end{bmatrix} \begin{bmatrix} x_n \\ y_n \\ z_n \end{bmatrix} = \begin{bmatrix} 0 \\ x_{n-1}z_{n-1} \\ x_{n-1}y_{n-1} \end{bmatrix} \tag{7}$$

where I is M order unit matrix, $D = (\xi_j'(t_i))_{i,j=1,2,\cdots M}$ is M order matrix, and the vector

$$\begin{aligned} [x_n, y_n, z_n] = {} & [x_n(t_1), x_n(t_2), \cdots, x_n(t_M), y_n(t_1), \\ & y_n(t_2), \cdots, y_n(t_M), z_n(t_1), z_n(t_2), \cdots, z_n(t_M)], \end{aligned} \tag{8}$$

The vector

$$\begin{aligned} [0, x_{n-1}z_{n-1}, x_{n-1}y_{n-1}] = {} & [0, \cdots, 0, x_{n-1}(t_1) \\ & \cdot z_{n-1}(t_1), x_{n-1}(t_2) \\ & \cdot z_{n-1}(t_2), \cdots, x_{n-1}(t_M)\, z_{n-1}(t_M)), x_{n-1}(t_1) \\ & \cdot y_{n-1}(t_1), x_{n-1}(t_2) \\ & \cdot y_{n-1}(t_2), \cdots, x_{n-1}(t_M)\, y_{n-1}(t_M))]. \end{aligned} \tag{9}$$

The first line of (7) is replaced separately by the equation of initial conditions (6) in turn.

So, we can get that $x_n(t_j), y_n(t_j), z_n(t_j)$, $(j = 1, 2, \cdots M)$ are approximate solution of (1) and (2).

3. Numerical Experiment

In this section, some numerical examples are studied to find some new chaotic behaviors and verify the existing chaotic dynamic behaviors. In Experiments 1–5, the accuracy of iteration control is $\varepsilon = 10^{-10}$, the initial iteration value $x_0 = y_0 = z_0 = 0$; $x_1 = y_1 = z_1 = T$, and for parameters a, b, c, and m see Table 1.

Experiment 1. We consider the model (1) with $a = -1.5, b = 5$ and the initial conditions $x(0) = 0, y(0) = 1, z(0) = 0$ [4].

We choose Chebyshev nodes, and the number of nodes $M = 40$. Figure 1 is obtained by using the current method with $c = 1$. Among them, (a) is the time series plot; (b) is the phase diagram of z; (c) is the three-dimensional space graph; (d) is the graph projected on (x, z)-plane; (e) is the graph projected on (y, z)-plane. Figures 2 and 3 are obtained by using the current method at $c = 10$ and $c = 100$, respectively. We can see that the fluctuation amplitude of x and y increases, while the fluctuation amplitude of z decreases with the increase of ρ. The corresponding graphs b, c, d, and e also have obvious changes.

Experiment 2. We consider the Lorenz-type system [6]

$$\begin{aligned} \frac{dx}{dt} &= a(y - x) + yz, \\ \frac{dy}{dt} &= cx - xz, \\ \frac{dz}{dt} &= -bz + xy \end{aligned} \tag{10}$$

We choose Chebyshev nodes, the number of nodes $M = 40$, and the parameters $a = 7, c = 5$ and the initial conditions $x(0) = 0, y(0) = 1, z(0) = 0$.

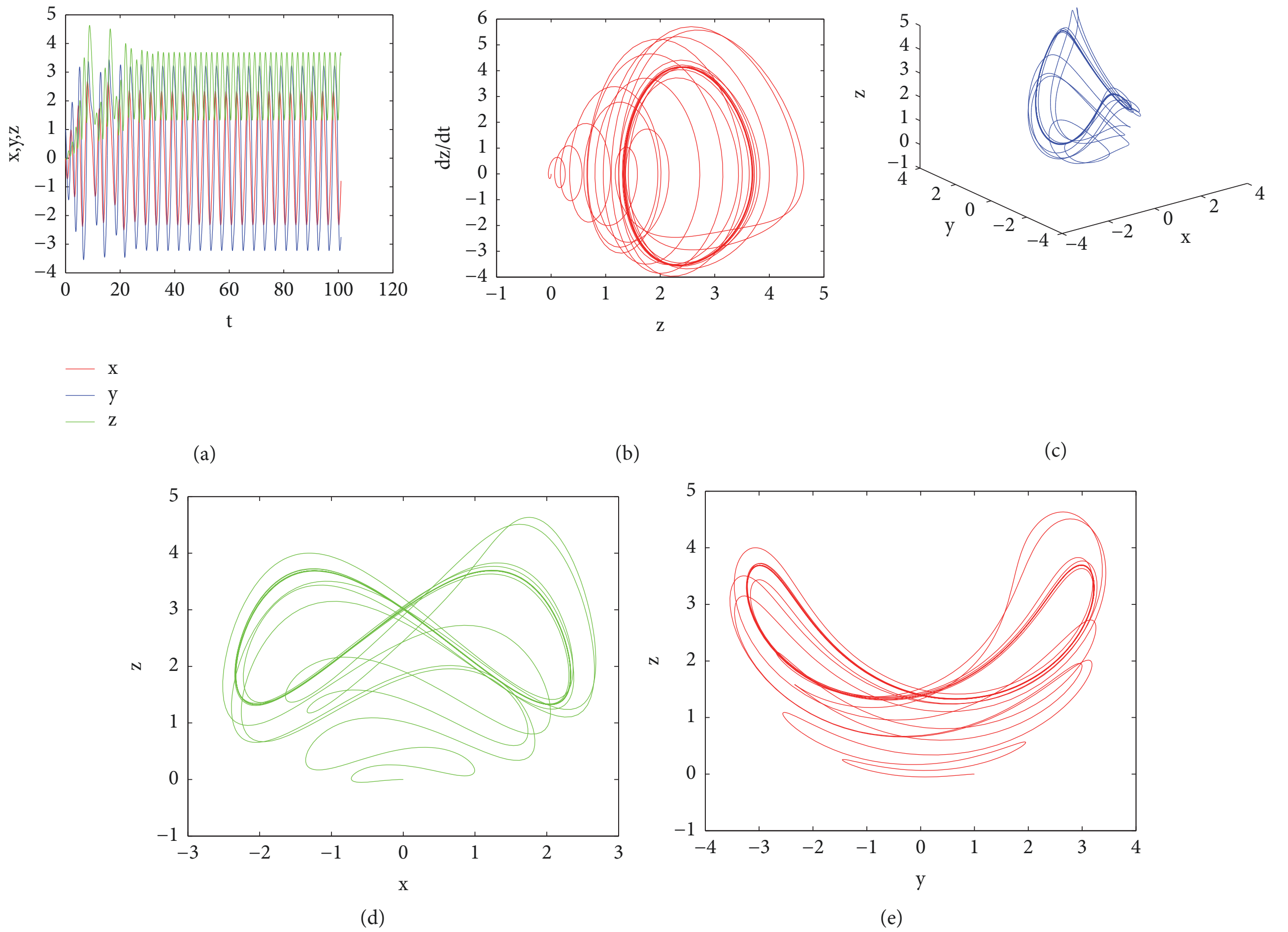

FIGURE 1: Lorenz system for Experiment 1 at $c = 1$: (a) time series plot; (b) phase diagram of z; (c) on the three-dimensional space; (d) projected on the (x, z)-plane; (e) projected on the (y, z)-plane.

TABLE 1: Parameters used in the Experiments 1–5.

Fig.	a	b	c	m
1	-1.5	5	1	
2	-1.5	5	10	
3	-1.5	5	100	
4	7	1	5	
5	7	2	5	
6	7	3	5	
8	10	15	1	
9	10	15	2	
10	10	15	3	
12	10	8/3	28	
13	0.5	-0.1	1.5	0.12

Figure 4 is strange attractors of chaotic system for Experiment 2 at $b = 1$ by using the current method. (a) is the graph projected on (x, y)-plane; (b) is the graph projected on (x, z)-plane; (c) is the graph projected on (y, z)-plane. Figure 7 is time series plots of chaotic system for Experiment 2 at different parameter value b. We can see that the frequency of fluctuations of x, y, and z accelerates obviously with the increase of b. When $b = 3$, the fluctuations of x, y, and z change obviously, and their fluctuations become smaller and smaller and finally stop at a certain value. Figures 5 and 6 are strange attractors of chaotic system for Experiment 2 by using the current method at $b = 2$ and $b = 3$ respectively.

Experiment 3. We consider the 3D autonomous chaotic Lorenz-type system [7]

$$\frac{dx}{dt} = a(y - x),$$
$$\frac{dy}{dt} = -xz - cy, \qquad (11)$$
$$\frac{dz}{dt} = -b + xy,$$

We choose Chebyshev nodes and the number of nodes $M = 60$ and the parameters $a = 10, b = 15$ and the initial conditions $x(0) = 10$, $y(0) = -0.2$, $z(0) = 0.75$.

Figure 8 is phase portraits of the 3D chaotic Lorenz type system for Experiment 3 at $c = 1$ by using the current method. (a) is the graph projected on (x, y)-plane; (b) is the graph

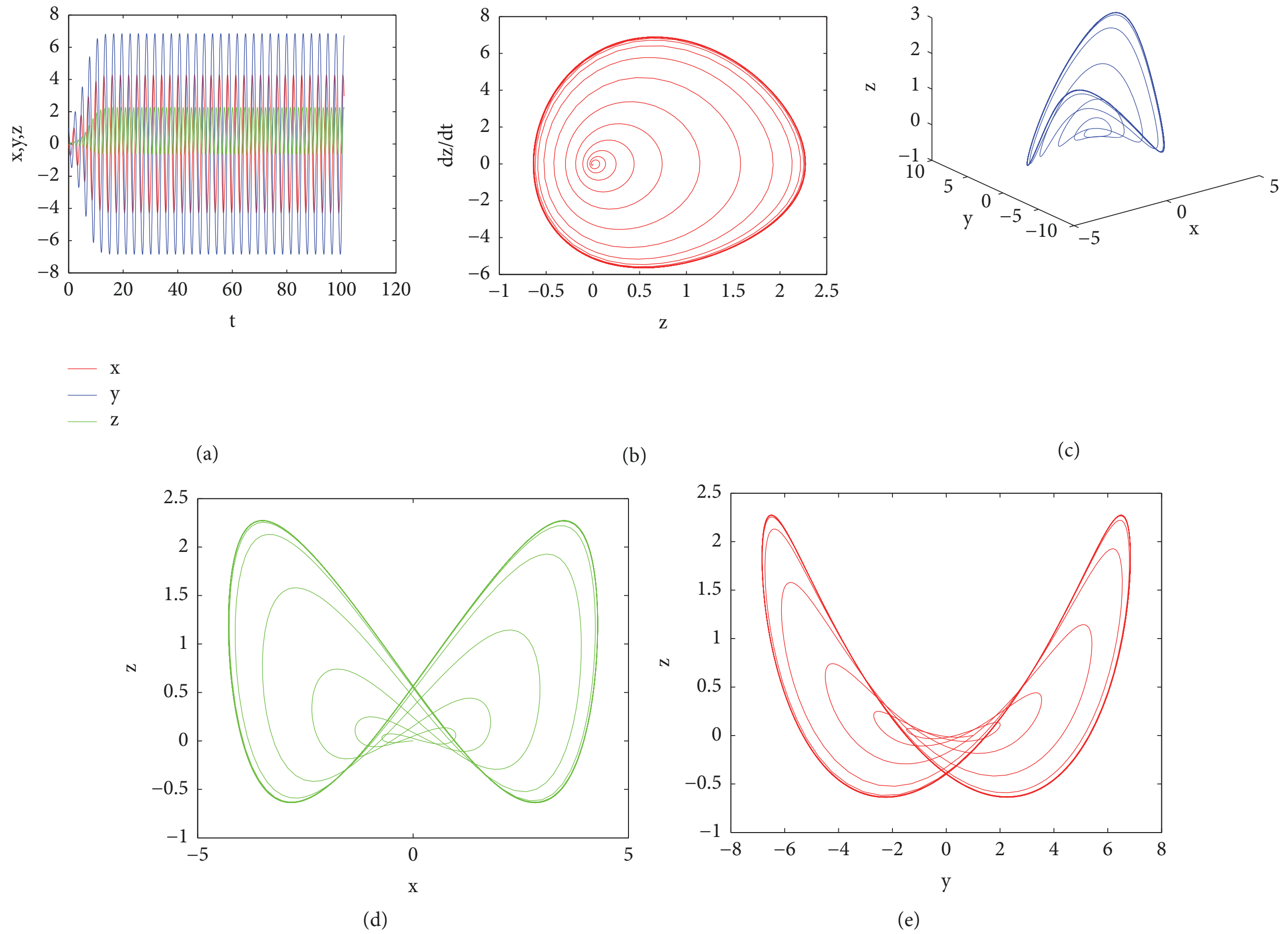

Figure 2: Lorenz system for Experiment 1 at $c = 10$: (a) time series plot; (b) phase diagram of z; (c) on the three-dimensional space; (d) projected on the (x, z)-plane; (e) projected on the (y, z)-plane.

projected on (x, z)-plane; (c) is the graph projected on (y, z)-plane. Figure 11 is time series plots of the 3D chaotic Lorenz type system for Experiment 3 at different parameter value c. We can see that the fluctuation range of y changes obviously with the increase of c. When $c = 1$, the fluctuation range of y is -5 to 15, and when $c = 3$, the fluctuation range of y is -15 to 5. Figures 9 and 10 are phase portraits of the 3D chaotic Lorenz type system for Experiment 3 by using the current method at $c = 2$ and $c = 3$, respectively.

Experiment 4. We consider the Lorenz system [5]

$$\begin{aligned} \frac{dx}{dt} &= -ax + ay, \\ \frac{dy}{dt} &= -ax - y - xz, \\ \frac{dz}{dt} &= -bz + xy - b(c + a), \end{aligned} \tag{12}$$

where a, b, and c are real parameters, which satisfy the following initial conditions:

$$\begin{aligned} x(0) &= 1, \\ y(0) &= 2, \\ z(0) &= 1 \end{aligned} \tag{13}$$

We choose Chebyshev nodes and the number of nodes $M = 40$. Figure 12 is obtained by using the current method with the parameters $a = 10$, $b = 8/3$, and $c = 28$. In Figure 12, (a) is the time series plot of x; (b) is the time series plot of z; (c) is the three-dimensional space graph; (d) is the graph projected on (x, y)-plane; (e) is the graph projected on (x, z)-plane; (f) is the graph projected on (y, z)-plane.

Experiment 5. We consider the new chaotic system [8]

$$\begin{aligned} \frac{dx}{dt} &= a(x - y), \\ \frac{dy}{dt} &= -4ay + xz + mx^3, \\ \frac{dz}{dt} &= -acz + x^3 y + bz^2, \end{aligned} \tag{14}$$

where x, y, and z are state variables and a, b, c, and m are real parameters, which satisfy the following initial conditions:

$$\begin{aligned} x(0) &= 0.5, \\ y(0) &= 0, \\ z(0) &= 0 \end{aligned} \tag{15}$$

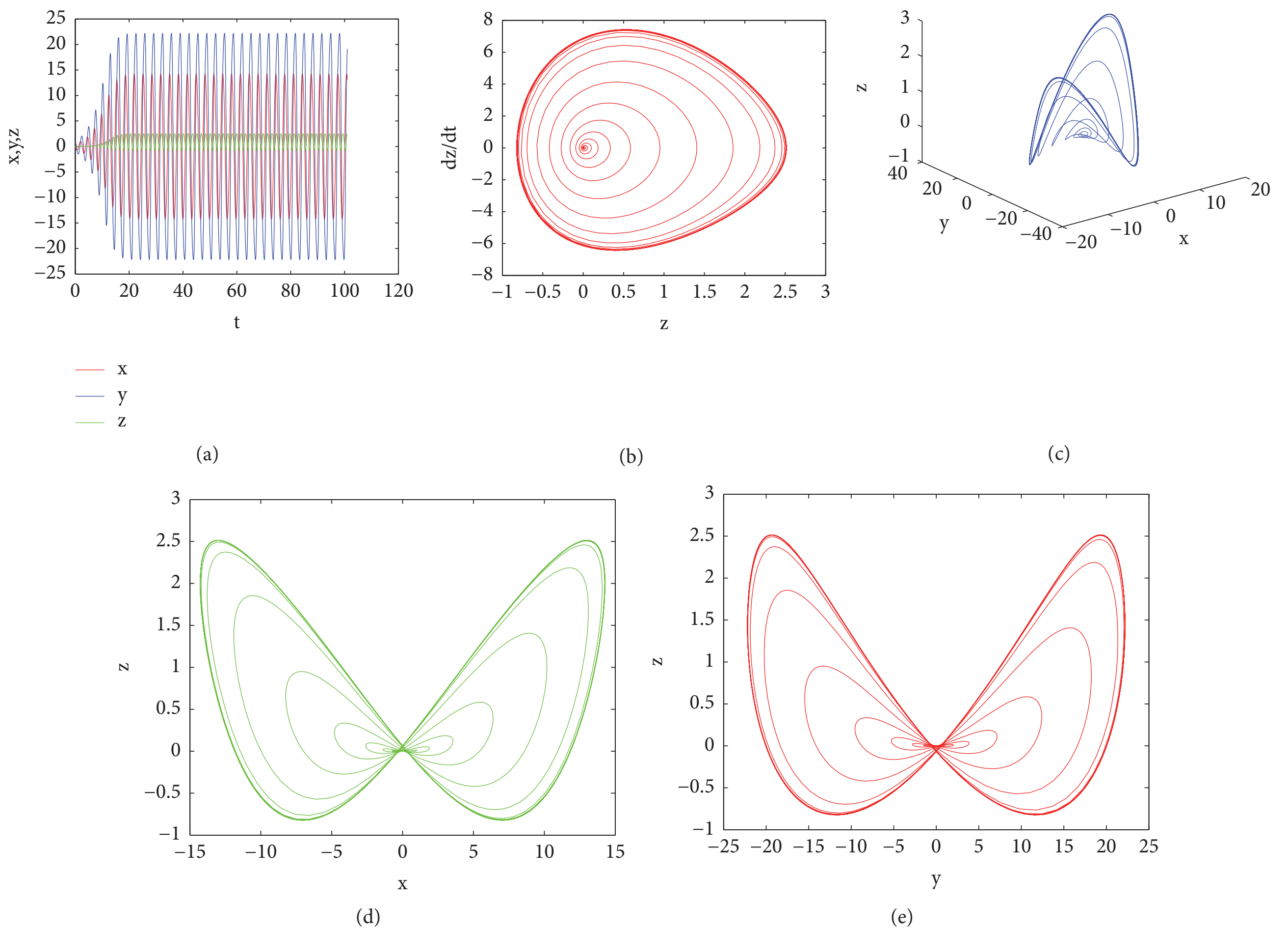

FIGURE 3: Lorenz system for Experiment 1 at $c = 100$: (a) time series plot; (b) phase diagram of z; (c) on the three-dimensional space; (d) projected on the (x, z)-plane; (e) projected on the (y, z)-plane.

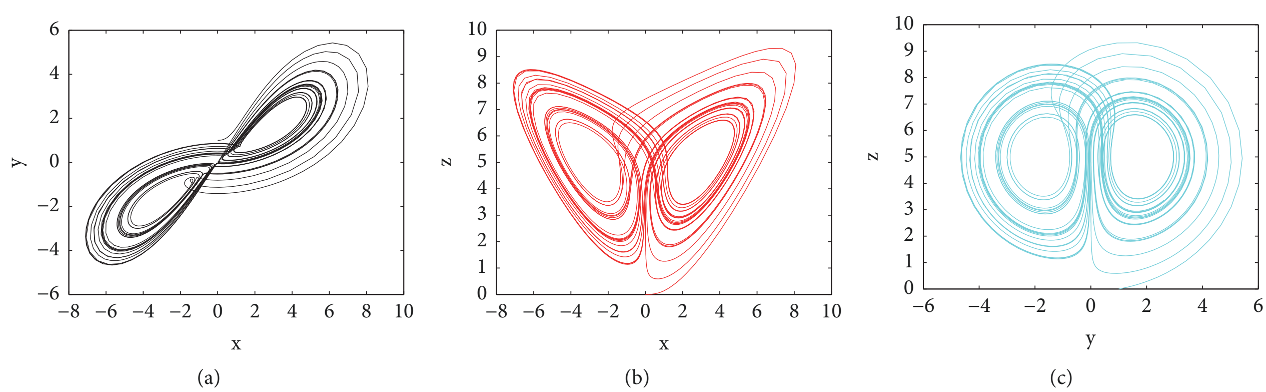

FIGURE 4: Strange attractors of chaotic system for Experiment 2 at $b = 1$: (a) (x, y)-plane; (b) (x, z)-plane; (c) (y, z)-plane.

We choose Chebyshev nodes and the number of nodes $M = 40$. Figure 13 is obtained by using the current method with the parameters $a = 0.5, b = -0.1$, $c = 1.5$, and $m = 0.12$. In Figure 13, (a) is the time series plot; (b) is the three-dimensional space graph; (c) is the graph projected on (x, y)-plane; (d) is the graph projected on (x, z)-plane; (e) is the graph projected on (y, z)-plane.

4. Conclusions and Remarks

In this paper, the Lorenz System has solved by using BLICM. These numerical experiments illustrate that the numerical results of the present method are the same as the experimental results.

All computations are performed by the MatlabR2017b software packages.

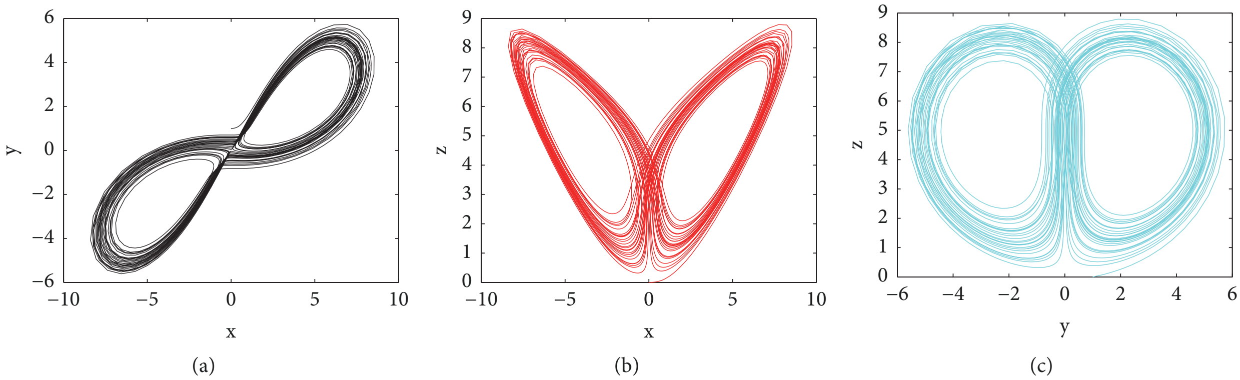

Figure 5: Strange attractors of chaotic system for Experiment 2 at $b = 2$: (a) (x, y)-plane; (b) (x, z)-plane; (c) (y, z)-plane.

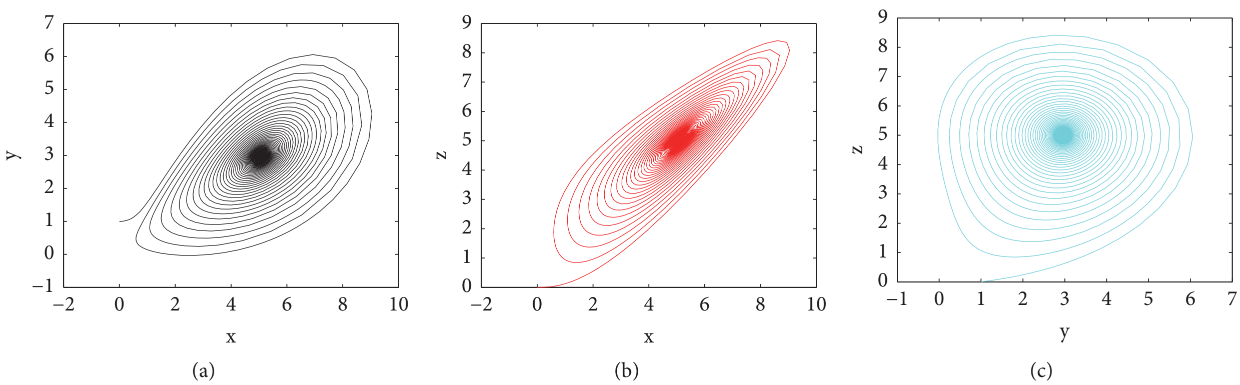

Figure 6: Strange attractors of chaotic system for Experiment 2 at $b = 3$: (a) (x, y)-plane; (b) (x, z)-plane; (c) (y, z)-plane.

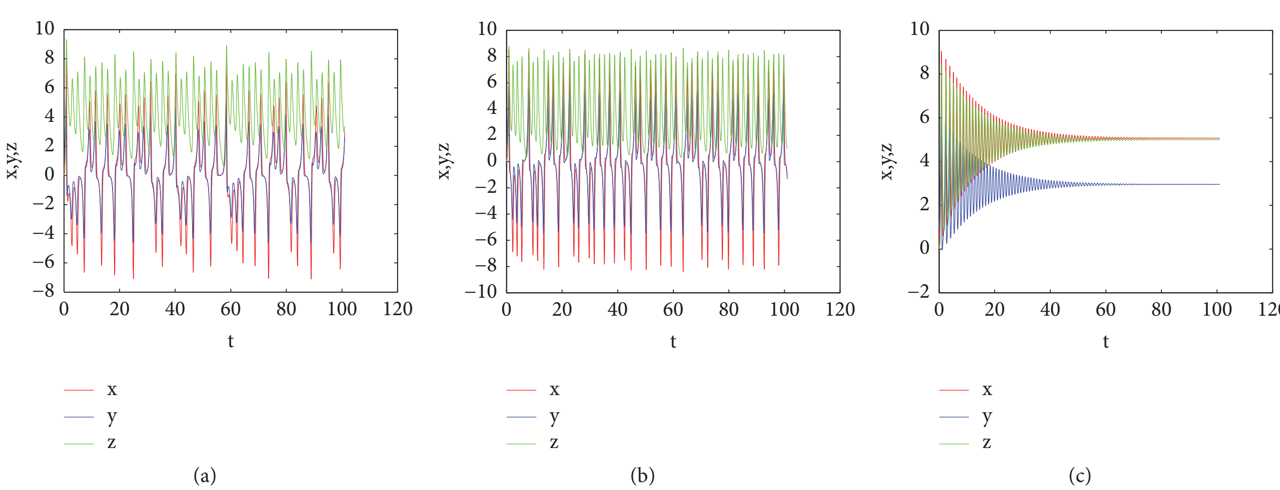

Figure 7: The time series plots of chaotic system for Experiment 2: (a) $b = 1$; (b) $b = 2$; (c) $b = 3$.

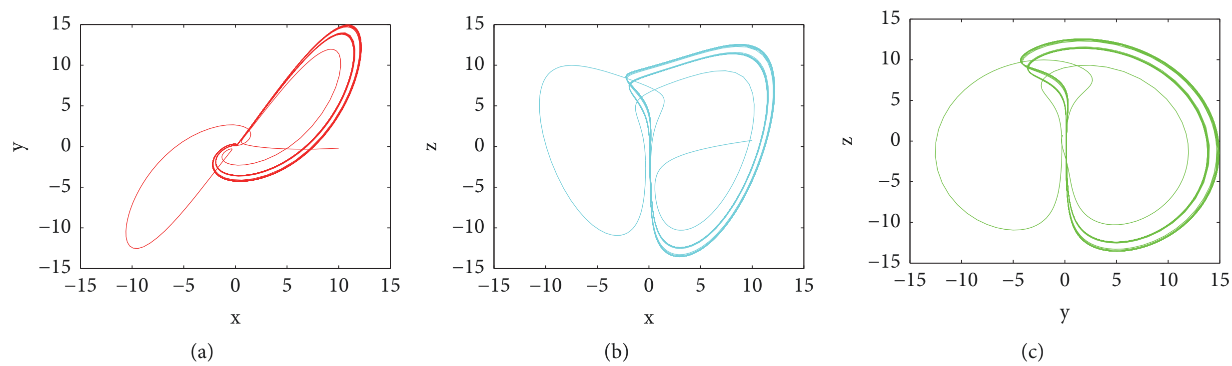

Figure 8: Phase portraits of the 3D chaotic Lorenz type system for Experiment 3 at $c = 1$: (a) (x, y)-plane; (b) (x, z)-plane; (c) (y, z)-plane.

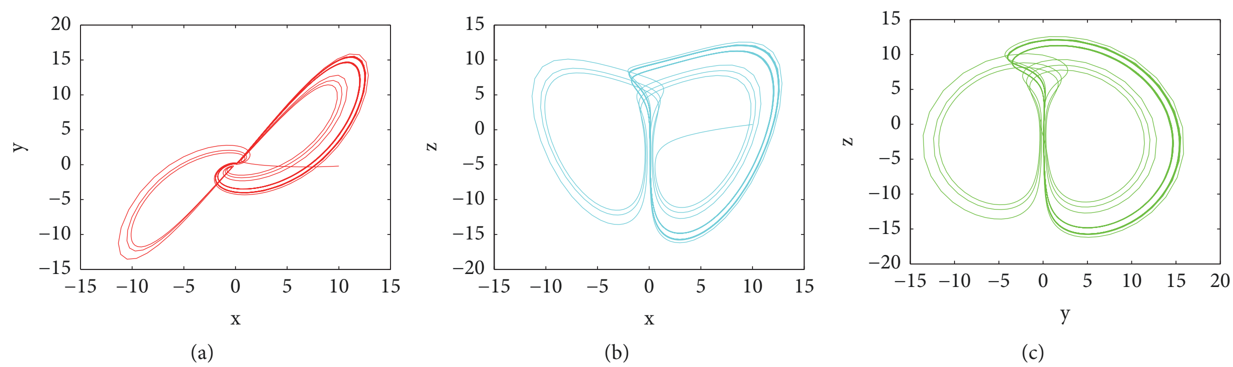

Figure 9: Phase portraits of the 3D chaotic Lorenz type system for Experiment 3 at $c = 2$: (a) (x, y)-plane; (b) (x, z)-plane; (c) (y, z)-plane.

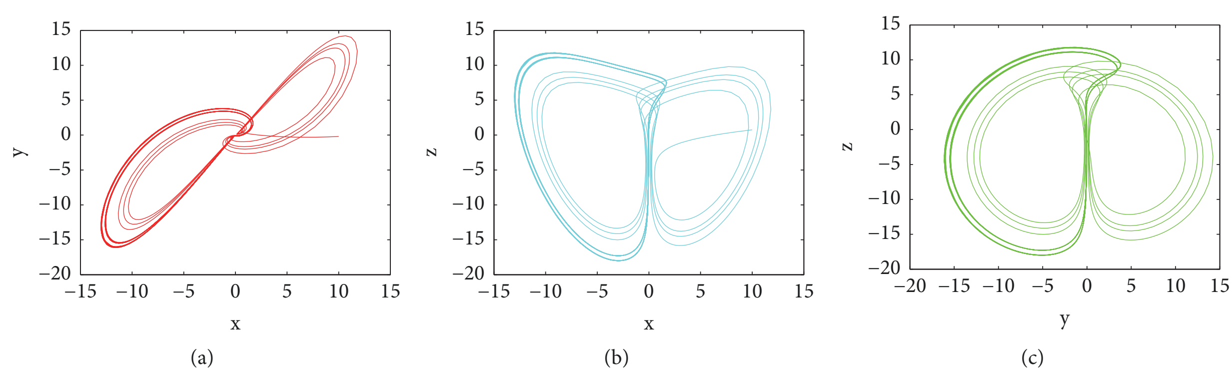

Figure 10: Phase portraits of the 3D chaotic Lorenz type system for Experiment 3 at $c = 3$: (a) (x, y)-plane; (b) (x, z)-plane; (c) (y, z)-plane.

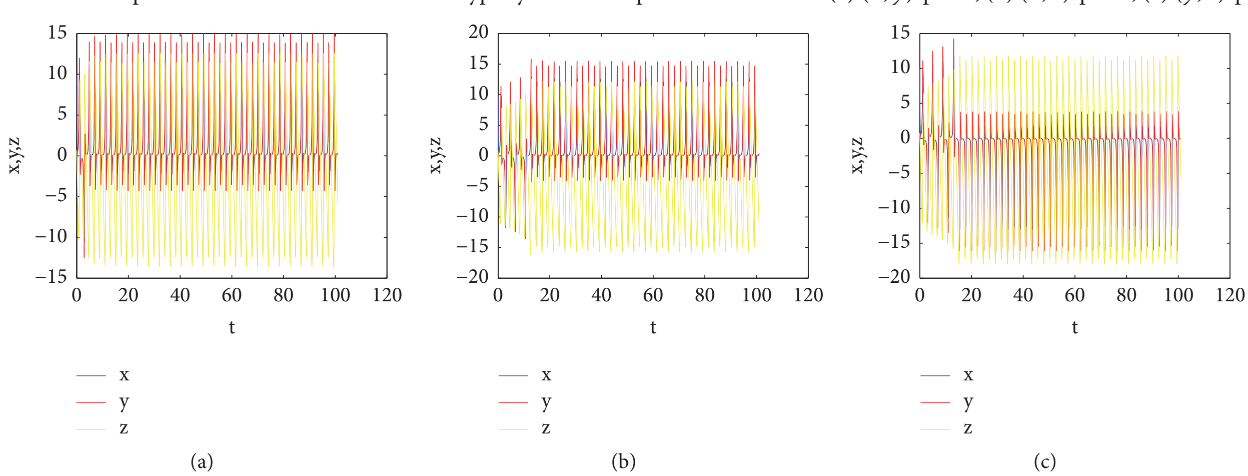

Figure 11: The time series plots of 3D autonomous chaotic Lorenz-type system for Experiment 3: (a) $c = 1$; (b) $c = 2$; (c) $c = 3$.

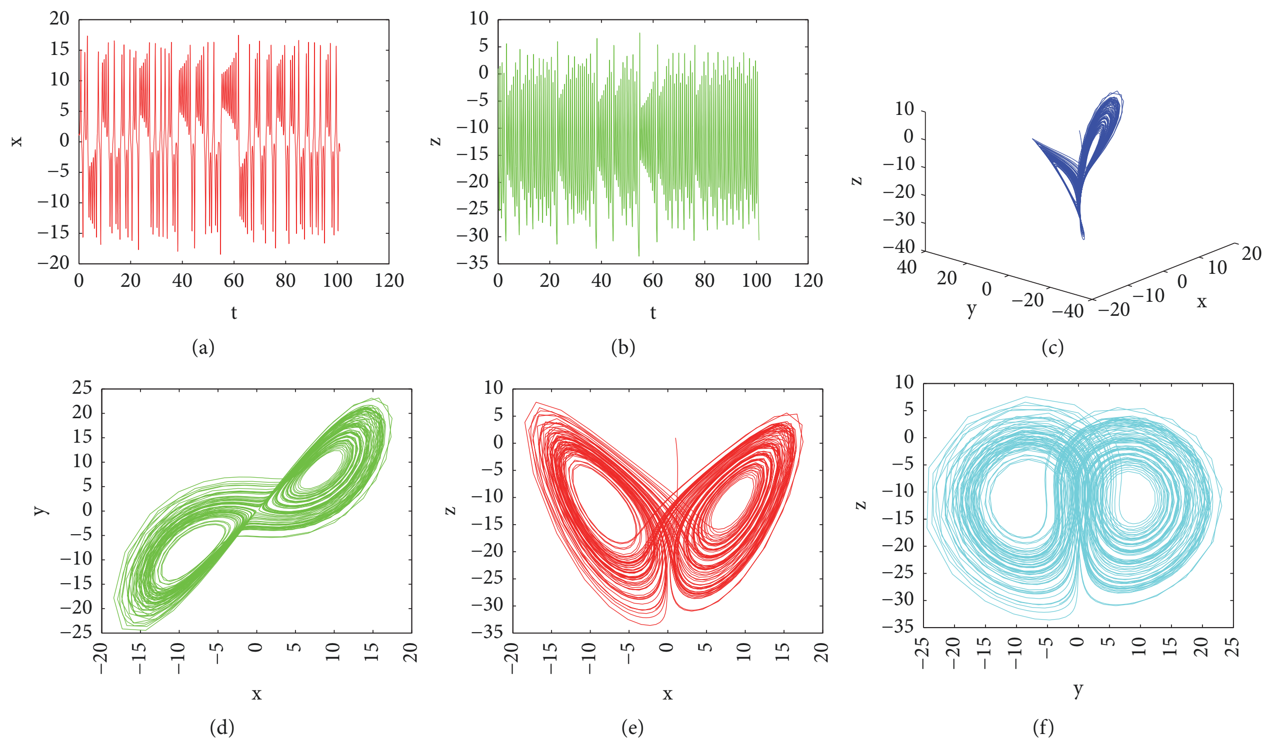

FIGURE 12: Lorenz system for Experiment 4 with $a = 10, b = 8/3, c = 28$: (a) time series plot of x; (b) time series plot of z; (c) on the three-dimensional space; (d) projected on the (x, y)-plane; (e) projected on the (x, z)-plane; (f) projected on the (y, z)-plane.

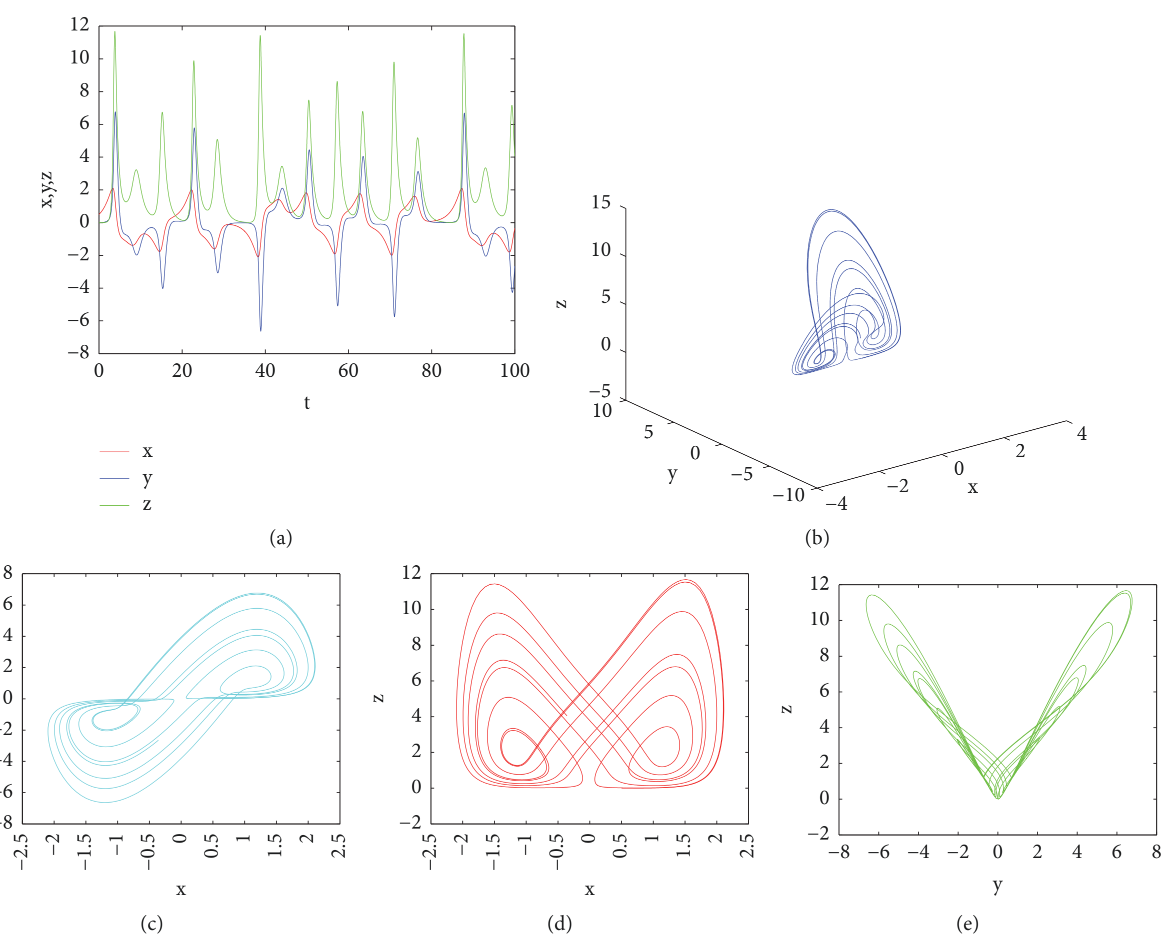

FIGURE 13: The new chaotic system for Experiment 5 with $a = 0.5, b = -0.1, c = 1.5, m = 0.12$: (a) time series plot; (b) on the three-dimensional space; (c) projected on the (x, y)-plane; (d) projected on the (x, z)-plane; (e) projected on the (y, z)-plane.

Data Availability

The data used to support the findings of this study are available from the corresponding author upon request.

Conflicts of Interest

The authors declare that there are no conflicts of interest regarding the publication of this article.

Acknowledgments

This paper is supported by the Natural Science Foundation of Inner Mongolia [2017MS0103], Inner Mongolia maker collaborative innovation center of Jining Normal University, and the National Natural Science Foundation of China [11361037].

References

[1] E. N. Lorenz, "Deterministic non-periodic flows," *Journal of the Atmospheric Sciences*, vol. 20, pp. 130–141, 1963.

[2] C. Sparrow, *The Lorenz Equations: Bifurcations, Chaos and Strange Attractors*, Springer, New York, NY, USA, 1982.

[3] A. N. Pchelintsev, "Numerical and physical modeling of the dynamics of the Lorenz system," *Numerical Analysis and Applications*, vol. 7, no. 2, pp. 159–167, 2014.

[4] A. Algaba, M. Merino, and A. J. Rodrguezluis, "Superluminal periodic orbits in the Lorenz system," *Communications in Nonlinear Science and Numerical Simulation*, vol. 39, pp. 220–232, 2016.

[5] K. Hayden, E. Olson, and E. S. Titi, "Discrete data assimilation in the Lorenz and 2D Navier-Stokes equations," *Physica D: Nonlinear Phenomena*, vol. 240, no. 18, pp. 1416–1425, 2011.

[6] C.-L. Li, J.-B. Xiong, and W. Li, "A new hyperchaotic system and its generalized synchronization," *Optik - International Journal for Light and Electron Optics*, vol. 125, no. 1, pp. 575–579, 2014.

[7] A. Khan and S. Singh, "Chaotic analysis and combination-combination synchronization of a novel hyperchaotic system without any equilibria," *Chinese Journal of Physics*, vol. 56, no. 1, pp. 238–251, 2018.

[8] A. Akgul, S. Hussain, and I. Pehlivan, "A new three-dimensional chaotic system, its dynamical analysis and electronic circuit applications," *Optik - International Journal for Light and Electron Optics*, vol. 127, no. 18, pp. 7062–7071, 2016.

[9] R. Barboza, "Dynamics of a hyperchaotic Lorenz system," *International Journal of Bifurcation and Chaos*, vol. 17, no. 12, pp. 4285–4294, 2007.

[10] J. He, "Variational iteration method for delay differential equations," *Communications in Nonlinear Science and Numerical Simulation*, vol. 2, no. 4, pp. 235-236, 1997.

[11] J.-H. He, "Variational iteration method for autonomous ordinary differential systems," *Applied Mathematics and Computation*, vol. 114, no. 2-3, pp. 115–123, 2000.

[12] J.-H. He and X.-H. Wu, "Construction of solitary solution and compacton-like solution by variational iteration method," *Chaos, Solitons & Fractals*, vol. 29, no. 1, pp. 108–113, 2006.

[13] J.-H. He, "Homotopy perturbation method: a new nonlinear analytical technique," *Applied Mathematics and Computation*, vol. 135, no. 1, pp. 73–79, 2003.

[14] X. Zhou, J. Li, Y. Wang, and W. Zhang, "Numerical simulation of a class of hyperchaotic system using barycentric Lagrange interpolation collocation method," *Complexity*, vol. 2019, Article ID 1739785, 13 pages, 2019.

[15] S. P. Li and Z. Q. Wang, *Barycentric Interpolation Collocation Method for Nonlinear Problems*, National Defense Industry Press, Beijing, China, 2015.

[16] S. P. Li and Z. Q. Wang, *High-Precision Non-Grid Center of Gravity Interpolation Collocation Method: Algorithm, Program and Engineering Application*, Science Press, Beijing, China, 2012.

[17] S. P. Li and Z. Q. Wang, "Barycentric interpolation collocation method for solving nonlinear vibration problems," *Noise Vibration Control*, vol. 28, pp. 49–52, 2018.

[18] Y. L. Wang, D. Tian, and Z. Y. Li, "Numerical method for singularly perturbed delay parabolic partial differention equations," *Thermal Science*, vol. 21, no. 4, pp. 1595–1599, 2017.

[19] F. Liu, Y. Wang, and S. Li, "Barycentric interpolation collocation method for solving the coupled viscous Burgers' equations," *International Journal of Computer Mathematics*, vol. 95, no. 11, pp. 2162–2173, 2018.

[20] H. Wu, Y. Wang, and W. Zhang, "Numerical solution of a class of nonlinear partial differential equations by using barycentric interpolation collocation method," *Mathematical Problems in Engineering*, vol. 2018, Article ID 7260346, 10 pages, 2018.

[21] H. Wu, Y. Wang, W. Zhang, and T. Wen, "The barycentric interpolation collocation method for a class of nonlinear vibration systems," *Journal of Low Frequency Noise, Vibration and Active Control*, 2019.

[22] H. Liu, J. Huang, Y. Pan, and J. Zhang, "Barycentric interpolation collocation methods for solving linear and nonlinear high-dimensional Fredholm integral equations," *Journal of Computational and Applied Mathematics*, vol. 327, pp. 141–154, 2018.

[23] R. Jiwari, S. Singh, and A. Kumar, "Numerical simulation to capture the pattern formation of coupled reaction-diffusion models," *Chaos, Solitons & Fractals*, vol. 103, pp. 422–439, 2017.

[24] J.-P. Berrut, "Baryzentrische Formeln zur trigonometrischen Interpolation (I)," *Zeitschrift Fur Angewandte Mathematik Und Physik*, vol. 35, pp. 91–105, 1984.

[25] J.-P. Berrut, "Rational functions for guaranteed and experimentally well conditioned global interpolation," *Computers & Mathematics with Applications*, vol. 15, no. 1, pp. 1–16, 1988.

[26] J.-P. Berrut and L. N. Trefethen, "Barycentric Lagrange interpolation," *SIAM Review*, vol. 46, no. 3, pp. 501–517, 2004.

[27] N. J. Higham, "The numerical stability of barycentric Lagrange interpolation," *IMA Journal of Numerical Analysis*, vol. 24, no. 4, pp. 547–556, 2004.

[28] W. F. Mascarenhas, "The stability of barycentric interpolation at the Chebyshev points of the second kind," *Numerische Mathematik*, vol. 128, no. 2, pp. 265–300, 2014.


Advances in
Operations Research
Advances in
Decision Sciences
Journal of
Applied Mathematics
The Scientific
World Journal
Journal of
Probability and Statistics
International
Journal of
Mathematics and
Mathematical
Sciences
Journal of
Optimization
Hindawi
Submit your manuscripts at
www.hindawi.com
International Journal of
Engineering
Mathematics
International Journal of
Analysis
Journal of
Complex Analysis
Advances in
Numerical Analysis
Mathematical Problems
in Engineering
International Journal of
Differential Equations
Discrete Dynamics in
Nature and Society
International Journal of
Stochastic Analysis
Journal of
Mathematics
Journal of
Function Spaces
Abstract and
Applied Analysis
Advances in
Mathematical Physics